Blood flow measurement and slow flow detection in retinal vessels with Joint Spectral and Time domain method in ultrahigh speed OCT

Blood flow measurement and slow flow detection in retinal vessels with joint Spectral and Time Domain method in ultrahigh speed OCT

I. Gorczynska[1], M. Szkulmowski[1], I. Grulkowski[1], A. Szkulmowska[1], D. Szlag[1], J.G. Fujimoto[2], A. Kowalczyk[1], M. Wojtkowski[1]

[1]Institute of Physics, Nicolaus Copernicus University in Torun, Poland
[2]Dept. of Electrical Engineering and Computer Science and Research Laboratory of Electronics, Massachusetts Institute of Technology, Cambridge, MA, USA

ABSTRACT

We present an application of the Joint Spectral and Time domain OCT (STdOCT) method for detection of wide range of flows in the retinal vessels. We utilized spectral/Fourier domain OCT (SOCT) technique for development of scan protocols for Doppler signal analysis. We performed retinal imaging in normal eyes using ultrahigh speed (200 000 axial scans/s) SOCT instrument with a CMOS camera. Various raster scan protocols were implemented for investigation of blood flow in the retina. Data analysis was performed using the method of joint Spectral and Time domain OCT (STdOCT). Detection of blood flow velocities ranging from several tens of mm/s to a fraction of mm/s was possible with scanning methods allowing for appropriate selection of time intervals between data taken for Doppler OCT analysis. Axial blood flow velocity measurement was possible in retinal vessels. Doppler OCT signal can be utilized as a contrast mechanism for visualization of retinal capillaries.

Keywords: Ultrahigh speed OCT, spectral/Fourier domain OCT, Doppler OCT, blood flow, retinal vasculature, retinal capillary

1. INTRODUCTION

Optical Coherence Tomography (OCT) has become a well established diagnostic technique in ophthalmology enabling high speed and high resolution imaging of the eye structure. However, there has been also a considerable interest in development of OCT methods for imaging of processes connected to functioning of the retina. One example are methods of blood flow detection in retinal vessels. Several OCT techniques enabling flow detection in the eye have been introduced up to date. The most widely used include the phase resolved / phase sensitive methods [1-7], techniques employing Doppler effect [8, 9] and resonant Doppler methods [10, 11]. Recently our group has introduced a Joint Spectral and Time domain OCT method (STdOCT) which can detect the flow based on the Doppler frequency shift visible in the OCT data as intensity beating signal [12].

Doppler OCT measurements rely on detection of the axial component (parallel to the scanning beam) of the flow velocity. In the retina, the magnitude of this velocity component can range from several tens of mm/s in the optic disc area, to a fraction of mm/s in the macular region. The velocity range which can be unambiguously measured with OCT methods is limited by the time interval Δt between consecutive Doppler OCT data (A-scans) and by the phase noise $\Delta\Phi_{err}$ [12-17]:

$$v_{\max} = \pm \frac{\lambda_0}{4 \cdot \Delta t}, \quad v_{\min} = \pm \frac{\lambda_0}{4 \cdot \Delta t} \cdot \frac{\Delta \Phi_{\mathrm{err}}}{\pi}, \tag{1}$$

where v_{max}, v_{min} are maximal and minimal axial velocity values, respectively, which can be measured with a given central wavelength λ_0 of the light emitted by the source used in the experiment. Central wavelength is measured in the flowing medium of the refractive index n, i.e. $\lambda_0=\lambda_0^{air}/n$. It is clear from equations (1) that decreasing Δt allows for faster flow velocity measurement. Slow flows can be measured if Δt is increased so that the slow phase changes (in phase sensitive methods) or the slow intensity changes of the Doppler beating signal (in Doppler OCT techniques) can be detected between consecutive OCT signals (A-scans). In other words, slow flow detection requires longer sampling times of the Doppler signal at a given point in the object thus enabling detection of the phase changes exceeding the phase noise $\Delta\Phi_{err}$ present during the imaging experiments. Measurements of the fast axial flow velocities became relatively easy with the advent of high speed OCT techniques. However, detection of slow flows is still challenging due

Ophthalmic Technologies XX, edited by Fabrice Manns, Per G. Söderberg, Arthur Ho, Proc. of SPIE Vol. 7550, 75501Y · © 2010 SPIE · CCC code: 1605-7422/10/$18 · doi: 10.1117/12.840020

to the phase noise considerations and long imaging times required for acquisition of the three dimensional data resulting in motion artifacts and discontinuity or loss of the flow information.

In this paper we present methods for axial flow velocity detection in retinal vessels including fast flows in the optic disk area as well as slow flows in the macular area. Detection of the wide range of velocities is possible with the development of specific scan protocols [18]. These protocols allow for adjustment of the time intervals between consecutive A-scans acquired for the Doppler signal analysis. Methods developed in this study enabled measurement of fast axial blood flow velocities in the large vessels in the optic disc area and visualization of the vasculature in the macular area including the capillary network. Combination of ultrahigh speed OCT imaging, specific scan protocols and STdOCT method allows for simultaneous three dimensional imaging of the retinal structure and flow in the retinal vessels.

2. MATERIALS AND METHODS

We performed the imaging experiments with a spectral/Fourier domain OCT laboratory instrument (Figure 1a). The instrument uses a classic fiber optic Michelson interferometer design. The object arm contains optical scanners and the optics for imaging of the retina. Dispersion compensation and light intensity attenuation is applied in the reference arm. As a light source we used a superluminescent diode (Superlum, SLD-351-HP2-DBUT-SM-PD) with 825nm central wavelength and 70nm full spectral width at half intensity maximum (FWHM). The measured axial resolution was 5.7μm in the air (~4.3μm in tissue). The transverse resolution was about 7μm. This value was estimated based on the possibility of imaging of cone photoreceptors in the parafoveal region (Figure 1b). The spectral OCT signal was detected using a custom made spectrometer with a linescan CMOS camera (Basler, Sprint) with 4096 pixels. The imaging speed depends on the camera settings: the number of active pixels and the exposure time [19]. We utilized 1024 camera pixels to achieve high speed read rates. The minimal exposure time was 3.4μs resulting in 4.7μs line period. Thus, the maximal achievable imaging speed was ~213 000 axial scans per second. The parameters of the instrument are summarized in Table 1.

Table 1. Parameters of the OCT instrument

Parameter	Value
Light source	SLD-351-HP2-DBUT-SM-PD, Superlum
Central wavelength	825nm
Axial resolution (in tissue)	~ 4.3 μm
Transverse resolution	~ 7 μm
Light power at the cornea	800 mW
Camera	Basler, Sprint, CMOS line scan
No. of active camera pixels	1024
Repetition time	4.7 μs
Maximum imaging speed	213 000 lines/s
Sensitivity	94 dB
Imaging depth in tissue	1.4 mm
Sensitivity roll-off over half/entire depth range	7dB / 20dB

Table 2. Parameters of the scan protocols

Scan protocol for	fast flow	slow flow
A-scans/B-scan	1100	250
B-scans	200	1000
Horizontal scan range	1.1 mm	1mm
Horizontal oversampling*	7	1.75
Vertical scan range	1 mm	1.1 mm
Vertical oversampling*	1.4	6.4
Repetition time	20 μs	4.7 μs
Imaging speed	50,000 A-scans/s	213,000 A-scans/s
Total imaging time	4.4 s	1.2 s
Time interval between consecutive Doppler data	20 μs	1.2 ms
Maximum measurable axial velocity	10.25 mm/s	0.17 mm/s

*Oversampling is defined as a ratio of the beam diameter to the scanning step size.

The flow detection was performed using the Joint Spectral and Time Domain OCT method [12] (Figure 2). The spectral OCT signal was acquired during raster scan with oversampling sufficient for the detection of the Doppler frequency shifts at a given transverse location in the object (the details of scan protocols are given in Table 2). For each such location two-dimensional Fourier transformation was performed. If Fourier transformation along the wavenumber axis is performed, a set of A-scans containing the structural information is generated at consecutive time intervals (top right panel in Figure 2a). If transformation along the time axis is performed then a set of Doppler frequency profiles at consecutive wavenumbers is obtained (bottom left panel in Figure 2a). If these transformations are performed one after the other (i.e. two-dimensional Fourier transformation is computed), depth velocity profile and structural information are retrieved for one object point and displayed in an A-scan (bottom right panel in Figure 2a). A set of A-scans obtained at

subsequent transverse locations at the object provides three dimensional OCT data with information about the structure and flows inside the object.

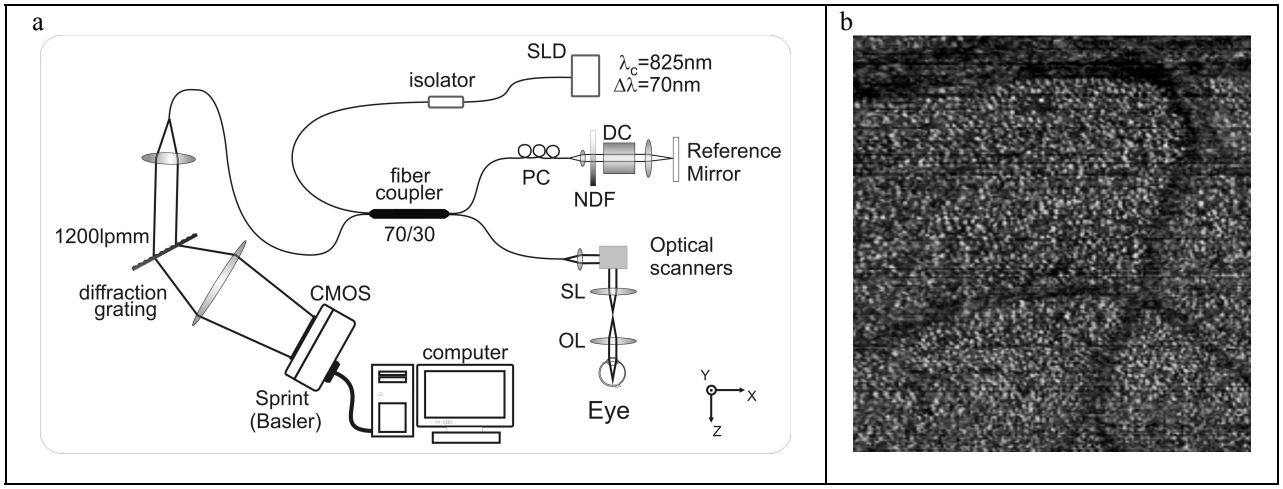

Figure 1. a. Schematics of the spectral/Fourier domain OCT instrument used for the study. SLD – superluminescent diode, PC – polarization controller, NDF – neutral density filter, DC – dispersion compensation, SL - scan lens, OL – ocular lens. b. Imaging of the cone photoreceptors in the parafovea allows to estimate the transverse resolution of the instrument to about 7μm. The location of the imaged area in the fundus is shown in Figure 4, label 6. Image size is 1 x 1.1 mm.

We performed the STdOCT measurements with application of two raster scan protocols (Table 2) allowing for detection of flow in different areas in the retina. The blood flow velocities in the optic disk area have large values (up to several tens of mm/s). Short time intervals between acquisitions of consecutive spectra are thus required for sufficient sampling of high Doppler frequencies. We achieved this by application of raster scan with oversampling in the fast axis direction. We then performed the STdOCT analysis using a sliding FFT window (top panel in Figure 2b). The number of spectra within the window depends on the degree of oversampling: all spectra must contain information about a given transverse location in the object. Fast flow images shown in this paper are obtained with FFT window containing 8 spectra. In the area closer to the macula, the axial velocity component has a small value (fraction of mm/s). Long sampling time intervals are thus recommended for flow detection. To meet this requirement we implemented raster scan protocol with oversampling in the slow scan axis direction (Table 2). The sliding FFT window contained spectra from 5 consecutive B-scans (image lines) acquired at time intervals equal to acquisition time of one image line (bottom panel in Figure 2b).

Imaging was performed in normal eyes. Imaging protocols for fast and slow flow detection were implemented in the parafoveal area and in the region of the optic disc. Images comparing the ability of both methods to detect flow in different retinal vessels were obtained, including the vasculature in the optic disc, the macula as well as the capillary network. The STdOCT images are compared with structural imaging of the vessels in projection OCT fundus images [20].

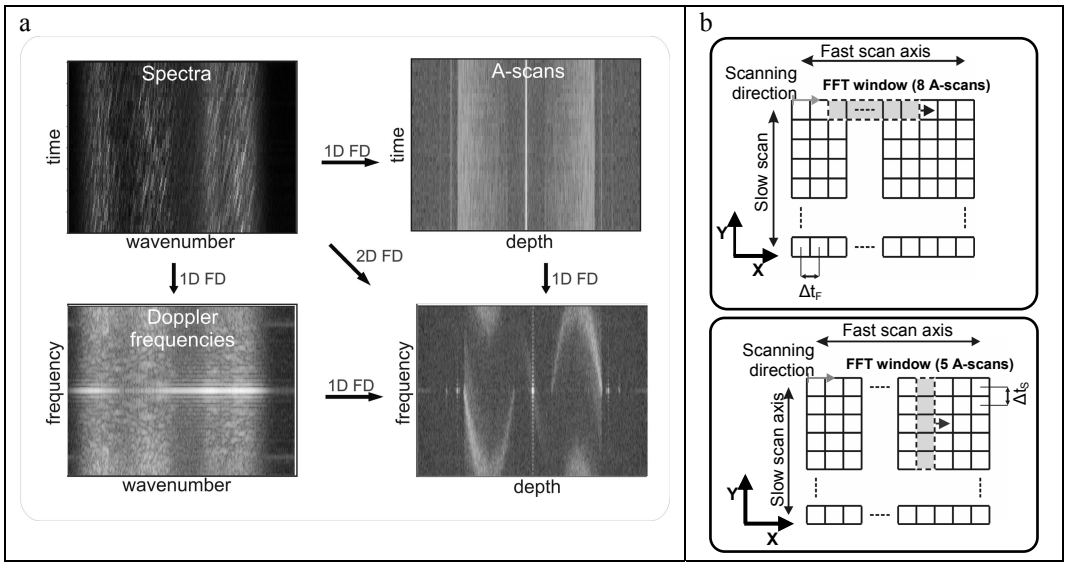

Figure 2. a. Illustration of the STdOCT method. Two consecutive Fourier transformations of the spectral fringe pattern acquired over time (top left) generate depth velocity profile and structural image (bottom right panel). The bottom right panel shows one A-scan across a glass capillary filled with flowing intralipid solution. The parabolic profile indicates the flow velocity distribution inside the capillary. b. Illustration of the scan protocols. Top panel - raster scan for fast flow measurements. Bottom panel - raster scan for slow flow detection. Grey rectangles - Fourier transform (FFT) windows for Doppler signal measurement. Δt_F = 20μs - time interval between two consecutive spectra in the FFT window for fast flow detection, Δt_S = 1.2 ms – time interval between two consecutive spectra in the FFT window for slow flow detection.

3. RESULTS

Results of application of scan protocols for fast and slow flow detection in the optic disk area are shown in OCT cross sectional images in Figure 3. The fast flow detection method allows for measurement of the axial flow velocity (Figure 3b). The velocity values are encoded in gray scale with gray levels from 0 (black) to 127 indicating direction of flow towards the incoming beam of light and gray levels from 128 to 255 (white) indicating flows along the beam. The value of 127 (grey color) indicates no flow (velocity value equal to 0) while 0 and 255 correspond to maximal velocities in opposite directions. In Figure 3b, a fragment of a vessel emerging from the optic disk is visible. In the left part of the vessel the blood is flowing towards the incoming beam of light (black color). After reaching the rim of the optic disc the orientation of the vessel changes and flow coinciding with the direction of the beam is detected (white color). In the part where the vessel orientation is perpendicular to the beam of light, the flow cannot be detected (grey color corresponding to velocity value equal to 0). Flow velocity profiles can be extracted at selected locations (Figure 3 e, f). Parabolic velocity distributions are visible in flow profiles extracted along A-scans as indicated by white vertical lines e and f in Figure 3b. The negative values of velocity correspond to flow towards the beam. Positive values indicate flow along the incoming beam of light.

Application of the slow flow scan protocol for imaging of large vessels in the optic disk area allows for the detection of flow but measurement of the axial flow velocity is not possible. Blood velocity in a vessel visible in Figure 3d largely exceeds the maximal value which can be measured unambiguously. As a results random distribution of flow velocities ranging from minimal to maximal values in both directions is obtained (Figure 3g). Although no quantitative information is available in this case, visualization of vasculature is still possible with utilization of flow as a natural contrast mechanism.

Results of three dimensional OCT flow imaging in areas indicated by rectangles in OCT fundus image (Figure 4) are shown in figures 5 and 6. In figure 5 vessels in the optic disc area are visualized with the fast flow (top row) and slow flow method (bottom row). OCT fundus images visualize two large vessels at the rim of the optic disk (Figures a and d). Figures b and e show the axial flow velocity maps. The method for fast flow detection provides quantitative information on flow velocities (Figure 4b) however small vessels are not visualized. Scan protocol for slow flow detection does not provide quantitative information but it can be utilized for detection of slow flows in small vessels (Figure 4e). In Figures

4c and f the information about axial velocity values was removed and flow was utilized only for visualization of vascular network. The method for slow flow detection reveals vessels which are not imaged with the fast flow detection method.

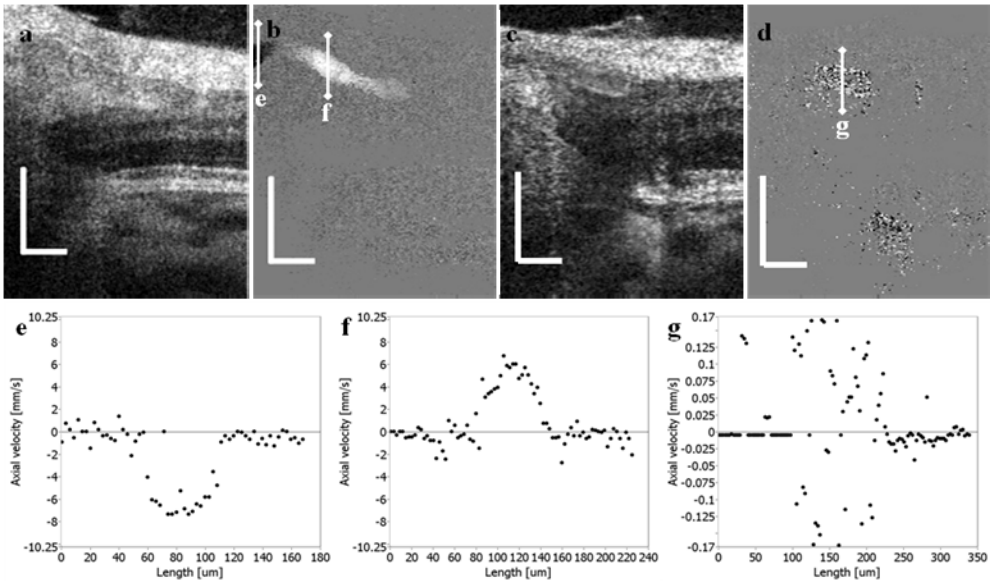

Figure 3. Cross sectional OCT images extracted from the three dimensional data (Figure 5) showing the flow in the optic disc area. a, b, e, f – fast flow detection method, c, d, g – slow flow detection method. a, c – structural images. b, d – flow images, white vertical lines indicate locations at which flow profiles shown in images e – g were extracted. Scale bars indicate 0.2mm x 0.2mm area.

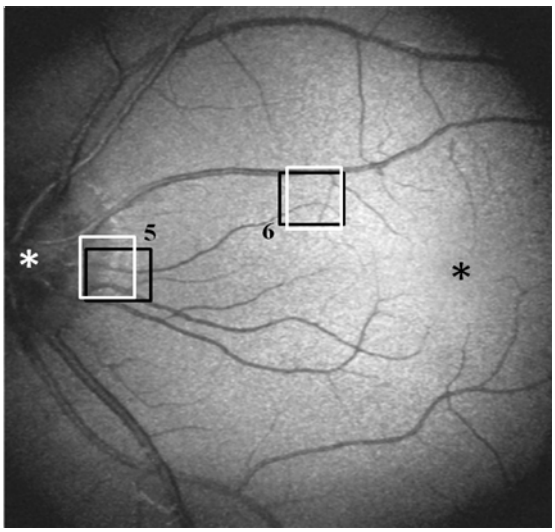

Figure 4. OCT fundus image indicating locations of the regions where three dimensional flow data was acquired. Black rectangles indicate location of data acquired with fast flow detection method. White rectangles show areas where scan protocols for slow flow detection were applied. 5, 6 – areas shown in Figures 5 and 6. White asterisk – optic disk. Black asterisk – fovea.

Figure 6 presents a series of images obtained in the parafoveal region of the retina. The top row shows images obtained with the scan protocol for fast flow detection. In bottom and middle rows results obtained with slow flow detection method are shown. In both cases structural imaging presented in OCT fundus images (Figures a and e) reveals several vessels present in this area of the retina. However, mapping of the flow velocity values generated with the fast flow detection method is not satisfactory. The orientation of vessels in this region of the fundus is almost perpendicular to the imaging beam of light and axial flow velocity values are small. Therefore fast flow detection method does not allow for

quantitative assessment of flow velocity. Visualization of the vasculature using flow as a contrast mechanism is not satisfactory with the fast flow detection method, either (Figure 6 b). Scan protocols for slow flow detection are therefore required. In Figures 6 f and g projection OCT fundus images [20] corresponding to the ganglion cell layer and the inner plexiform layer (Figure 6f) and to the inner nuclear layer and outer plexiform layer (Figure 6g) are presented. Highly scattering vessels are well visualized in the low scattering tissue (e.g. nuclear layer) allowing for visualization of the vascular network down to the capillary level (Figure 6g). However, small vessels located in the highly scattering tissue (e.g. plexiform layers) are poorly visualized (Figure 6f). STdOCT technique with application of slow flow detection method allows for detection of such vessels (Figure 6i) taking advantage of flow as a natural contrast mechanism. STdOCT imaging of the capillary network in the inner nuclear layer and in the outer plexiform layer is comparable with the projection OCT method.

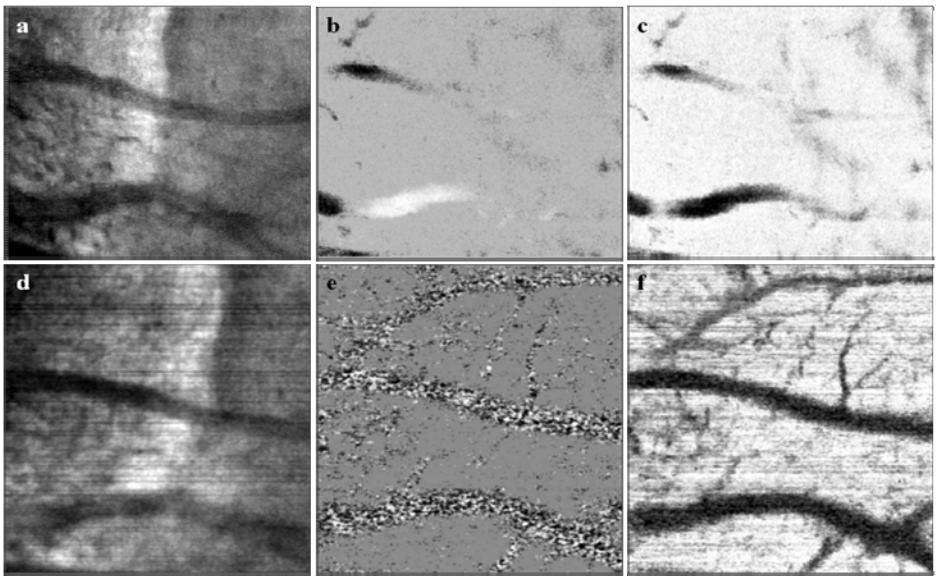

Figure 5. Three dimensional STdOCT imaging of flow in the optic disk area. Top row – images obtained with the fast flow detection method. Bottom row – images obtained with the slow flow detection method. a, d – OCT fundus images obtained by the axial summation of the 3-D OCT data. b, e – flow maps; gray scale encodes flow values: 0 (black) to 127 (grey) – flow towards the incoming beam of light, 128 (grey) - 255 (white) – flow along the incoming beam of light. c, f – visualization of vasculature achieved by utilization of flow as a natural contrast mechanism; quantitative information was removed, black indicates flow, white – no flow detected. Sizes of the images: a – c - 1.1mm x 1mm, d – f – 1mm x 1.1mm.

4. CONCLUSIONS

Results obtained in different areas in the retina with various scan protocols show the possibility of detection of flow with velocities ranging from several tens of mm/s to several tenths of mm/s. It is possible to utilize the flow as a natural contrast mechanism not only for imaging of large vessels in the proximity of the optic disk but also for the detection of capillary network in the macular region. However, if the goal is the velocity measurement, design of advanced scan protocols is required. Scan methods should specifically target Doppler shift frequencies characteristic of blood flow in given retinal regions. Implementation of such protocols is possible with application of ultrahigh speed OCT imaging. Combination of ultrahigh speed OCT detection and advanced method of signal analysis such as STdOCT allows for simultaneous three dimensional imaging of the retinal structure and flow in the retinal vessels.

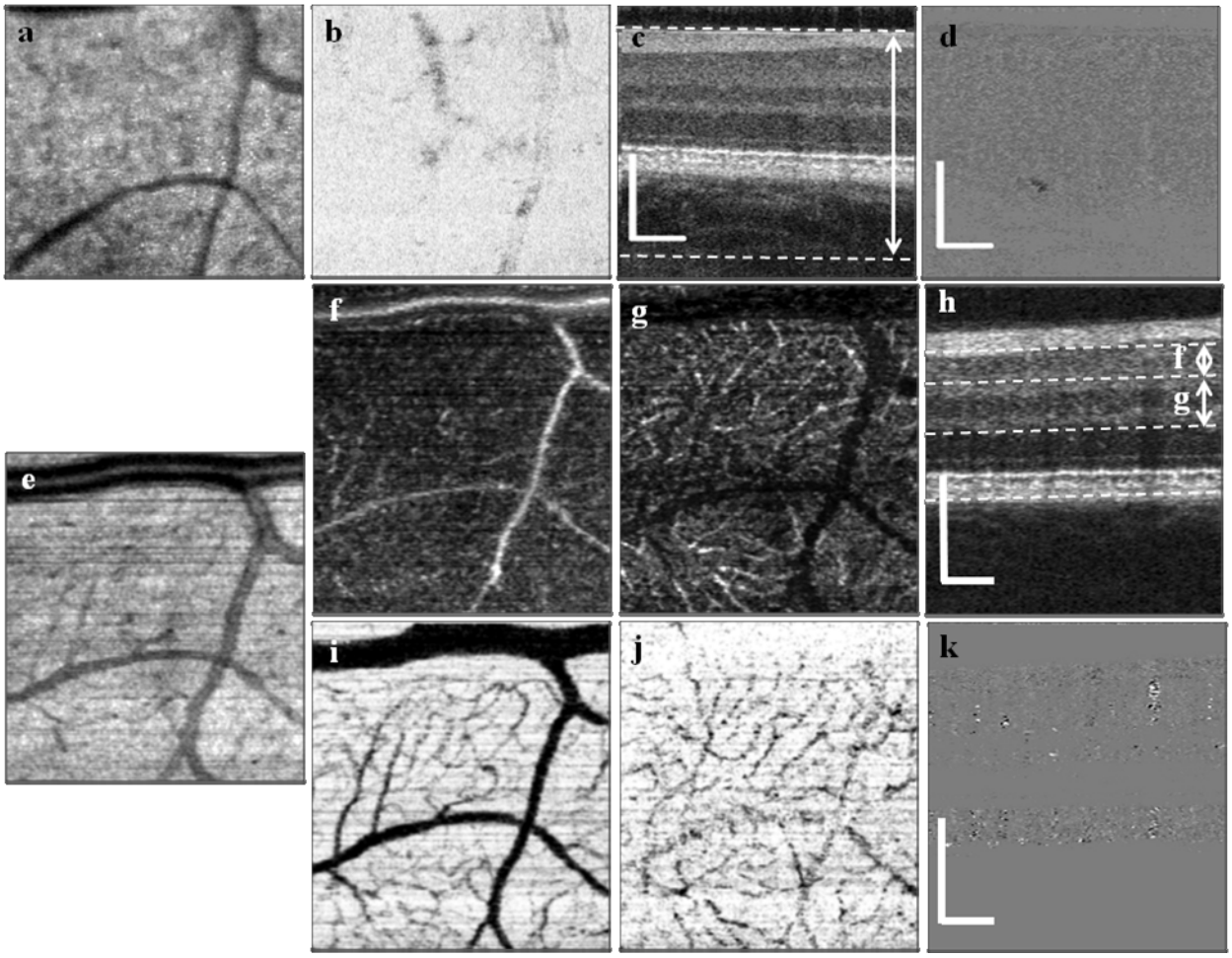

Figure 6. Three dimensional STdOCT imaging of flow in the macular area of the retina. Top row – images obtained with the fast flow detection method. Bottom and middle rows – images obtained with the slow flow detection method. a, e – OCT fundus images. b, i, j – visualization of the vasculature with utilization of flow as a natural contrast mechanism. c - structural cross-sectional image; white arrow and the dashed lines indicate the depth range used to generate image b. d – example cross-sectional flow image extracted from the 3-D data set: no vessels are visible in the retina, however blood flow is detected in the choroid (black patch), h – structural OCT cross-section: dashed lines and arrows indicate depth ranges used to generate images f, i and g, j. k – example cross-sectional flow image: random distribution of flow values (black and white pixels) indicates location of the small vessels. Scale bars indicate 0.2mm x 0.2 mm area. Size of images a and b is 1.1mm x 1mm. Size of images e – g, i, j is 1mm x 1.1 mm.

ACKNOWLEDGEMENTS

I. Gorczynska acknowledges the support from Polish Ministry of Science and Higher Education, grant No. 2076/B/H03/2009/37. M. Szkulmowski acknowledges support of Foundation for Polish Science (START 2009). M. Wojtkowski acknowledges support from the European Heads of Research Councils and the European Science Foundation: EURYI-01/2008-PL, EURYI-05-102-ES.

REFERENCES

[1] Yazdanfar, S., Rollins, A. M.Izatt, J. A., "Imaging and velocimetry of the human retinal circulation with color Doppler optical coherence tomography," Optics Letters, 25, 1448-1450 (2000).

[2] Bachmann, A. H., Michaely, R., Lasser, T.Leitgeb, R. A., "Dual beam heterodyne Fourier domain optical coherence tomography," Optics Express, 15, 9254-9266 (2007).
[3] Leitgeb, R. A., Schmetterer, L., Drexler, W., Fercher, A. F., Zawadzki, R. J.Bajraszewski, T., "Real-time assessment of retinal blood flow with ultrafast acquisition by color Doppler Fourier domain optical coherence tomography," Optics Express, 11, 3116-3121 (2003).
[4] Makita, S., Hong, Y., Yamanari, M., Yatagai, T.Yasuno, Y., "Optical coherence angiography," Optics Express, 14, 7821-7840 (2006).
[5] Wehbe, H., Ruggeri, M., Jiao, S., Gregori, G., Puliafito, C. A.Zhao, W., "Automatic retinal blood flow calculation using spectral domain optical coherence tomography," Optics Express, 15, 15193-15206 (2007).
[6] Werkmeister, R. M., Dragostinoff, N., Pircher, M., Götzinger, E., Hitzenberger, C. K., Leitgeb, R. A.Schmetterer, L., "Bidirectional Doppler Fourier-domain optical coherence tomography for measurement of absolute flow velocities in human retinal vessels," Opt. Lett., 33, 2967-2969 (2008).
[7] White, B. R., Pierce, M. C., Nassif, N., Cense, B., Park, B. H., Tearney, G. J., Bouma, B. E., Chen, T. C.de Boer, J. F., "In vivo dynamic human retinal blood flow imaging using ultra-high-speed spectral domain optical Doppler tomography," Optics Express, 11, 3490-3497 (2003).
[8] Wang, Y., Bower, B. A., Izatt, J. A., Tan, O.Huang, D., "Retinal blood flow measurement by circumpapillary Fourier domain Doppler optical coherence tomography," Journal of Biomedical Optics, 13, 064003-064009 (2008).
[9] An, L., Wang, R. K., "In vivo volumetric imaging of vascular perfusion within human retina and choroids with optical micro-angiography," Opt. Express, 16, 11438-11452 (2008).
[10] Bachmann, A. H., Villiger, M. L., Blatter, C., Lasser, T.Leitgeb, R. A., "Resonant Doppler flow imaging and optical vivisection of retinal blood vessels," Optics Express, 15, 408-422 (2007).
[11] Michaely, R., Bachmann, A. H., Villiger, M. L., Blatter, C., Lasser, T.Leitgeb, R. A., "Vectorial reconstruction of retinal blood flow in three dimensions measured with high resolution resonant Doppler Fourier domain optical coherence tomography," J Biomed Opt, 12, 041213 (2007).
[12] Szkulmowski, M., Szkulmowska, A., Bajraszewski, T., Kowalczyk, A.Wojtkowski, M., "Flow velocity estimation using joint Spectral and Time Domain Optical Coherence Tomography," Optics Express, 16, 6008-6025 (2008).
[13] Tao, Y. K., Kennedy, K. M.Izatt, J. A., "Velocity-resolved 3D retinal microvessel imaging using single-pass flow imaging spectral domain optical coherence tomography," Opt. Express, 17, 4177-4188 (2009).
[14] Szkulmowska, A., Szkulmowski, M., Kowalczyk, A.Wojtkowski, M., "Phase-resolved Doppler optical coherence tomography - limitations and improvements," Optics Letters, 33, 1425-1427 (2008).
[15] Park, B. H., Pierce, M. C., Cense, B., Yun, S. H., Mujat, M., Tearney, G., Bouma, B.de Boer, J., "Real-time fiber-based multi-functional spectral-domain optical coherence tomography at 1.3 μm," Optics Express, 13, 3931-3944 (2005).
[16] Schmoll, T., Kolbitsch, C.Leitgeb, R. A., "Ultra-high speed volumetric tomography of human retinal blood flow: erratum," Opt. Express, 17, 6025-6025 (2009).
[17] Schmoll, T., Kolbitsch, C.Leitgeb, R. A., "Ultra-high-speed volumetric tomography of human retinal blood flow," Opt. Express, 17, 4166-4176 (2009).
[18] Grulkowski, I., Gorczynska, I., Szkulmowski, M., Szlag, D., Szkulmowska, A., Leitgeb, R. A., Kowalczyk, A.Wojtkowski, M., "Scanning protocols dedicated to smart velocity ranging in Spectral OCT," Opt. Express, 17, 23736-23754 (2009).
[19] Potsaid, B., Gorczynska, I., Srinivasan, V. J., Chen, Y., Jiang, J., Cable, A.Fujimoto, J. G., "Ultrahigh speed Spectral / Fourierdomain OCT ophthalmic imaging at70,000 to 312,500 axial scans per second," Opt. Express, 16, 15149-15169 (2008).
[20] Gorczynska, I., Srinivasan, V. J., Vuong, L. N., Chen, R. W. S., Liu, J. J., Reichel, E., Wojtkowski, M., Schuman, J. S., Duker, J. S.Fujimoto, J. G., "Projection OCT fundus imaging for visualising outer retinal pathology in non-exudative age-related macular degeneration," Br J Ophthalmol, 93, 603-609 (2009).